Momentum Matrix Elements of Quantum Dot Structures with and without Applied Electric Field

Haneen Akram, Ektefaa Rehman and Amin Habbeb Al-Khursan
Nassiriya Nanotechnology Research Laboratory (NNRL), Science College, Thi-Qar University, Nassiriyah, Iraq.

Received Date: 28 / 3 / 2017
Accepted Date: 25 / 5 / 2017

الخلاصة

وضع نموذج للعناصر القطرية وغير القطرية لمصفوفة الزخم لتركيب النقط الكمية بتأثير وبدون تأثير المجال الكهربائي المسلط لمنطقتي النقط الكمية: طبقة النقط الكمية وطبقة الترطيب. تم اعتبار دالة الموجة المتعامدة المعايرة لطاقات طبقة الترطيب في مستوي الطبقة.

بينما كان هناك بعد محدد يعطي أعظم زخم للعناصر غير القطرية فإن العناصر القطرية تزداد مع البعد. بعض العناصر القطرية تزداد مع المجال وبعضها الآخر يقل.

الكلمات المفتاحية

النقط الكمية، طبقة الترطيب، عناصر مصفوفة الزخم القطرية، عناصر مصفوفة الزخم غير القطرية.

Abstract

Diagonal and off-diagonal momentum matrix elements of quantum dot (QD) structures with and without applied electric field were modeled for the structure layers; QD layer and wetting layer (WL). Orthogonal zed plane-wave (OPW) was considered for in-plane WL states.

While there is a definite size gives maxima for off-diagonal elements, the on-diagonal elements under applied field increases with size. Some of on-diagonal elements increase with field while some other decreases.

Keywords

Quantum dots, Wetting layer, Momentum matrix element.

1. Introduction

In the past few years with the advances in micro-fabrication has made it possible to fabricate zero-dimensional quantum dots (QDs) with fully controlled shape and size. QDs exhibit discrete energy states confine, in all three-space dimensions, charge carriers with wavelike characteristics. The study of the charged carriers confined in QDs has generated great expectation due to its potential applications in electronic and optoelectronic devices. The main problem in the research into the optical properties of QDs is to obtain the energy levels of the confined carriers and understanding it, which reflects the quantum size and shape effects [1]. An Ana lytical relations for energy sub band calculations were done earlier which makes it easy to study different applications of these structures under the applied electric field. These calculations give good results compared with the experiment and numerical calculations. More details in references [2-6].

QD structure composed of QD layer which is grown in two-dimensional quantum-well wetting layer (WL). The problem of transition between two different states takes an important attention in the structure have dissimilar regions as in QD structure. It is solved either by considering an infinite potential QD region or by considering the orthogonalization between these two types of states. The practical solution must consider both finite potential and orthogonality between different states.

This work deals with momentum matrix element of transitions in QD structure including both WL-WL, WL-QD, and QD-QD under and without applied electric field. Orthogonalized plane wave (OPW) is considered for WL-QD transitions. Relation for diagonal and off-diagonal elements of momentum are stated. Calculations of momentum are presented. It is found that WL momenta are the smallest ones. The effects of mediated states were predicted.

2. The problem of WL-QD

It is well known experimentally, and theoretically that QD structures contains two types of transitions. They are; inter dot (QD-QD) transitions and WL-QD transitions. These transitions are completely different. It is found that WL was coupled to ground state (GS) via excited state (ES) through slow WL-QD ES transitions while QD dynamics are dominated by fast electron dynamics between ES and GS, i.e. inter dot transitions [7]. This requires a specific formulation of these transitions.

M. Abdullah et. al. proposed ladder plus Y-configuration in double QD structure under applied electric field [8]. In their calculation of momentum matrix element between WL-QD states, the system wave function is separated into two components for the in-plane and the z-components. The z-component is described by Airy function since the studied structure is under applied electric field. They used Bessel functions to describe the in-plane

wave function in the disk instead of considering the simple two-dimensional harmonic oscillator (SHO), as the eign function of the QDs, used by Malic et. al. [9] which is far from the practical description of QDs, because of the equi spaced distant energy states in harmonic oscillator, which is impossible to attain in growing processes of QDs.

Although Abdullah solution [8] was good to solve the problem, but there is still a main point to be formulated. Due to the difference between QDs and WL, it requires the use of orthogonalized plane wave (OPW) for the in-plane WL states. This work, thus, contains the required development. It considers the Bessel function in the description of in-plane QD states in addition to orthogonalized plane wave in the description of WL states.

3. The Momentum Matrix under the applied electric field

3.1. Formulation of WL-QD transition:

In addition to inter dot transitions, WL-QD transitions between QD sub bands and a quasi-continuum WL state at higher energy were considered. These transitions are principal in the QD response.

In the WL, the in-plane wave function can be represented by plane waves multiplied by the state due to the confinement results from the barrier of finite height in the perpendicular direction. For WL-QD transitions, orthogonality between WL-QD states is required which results in additional oscillations [10]. This situation may represented by orthogonalized plane wave (OPW). The work of Nielsen et. al. was pioneer in this field but they, also, use SHO type for wave functions in QD [10].

In this work, for the QD wave function, the z-component is described by the Airy function since the studied structure is under the applied electric field. Then, in the QD structure the wave function is,

$$\varphi_{QD}(\vec{r}) = \varphi_{QD}(\vec{\rho})\ \zeta(\vec{z})u(\vec{r}) \qquad (1)$$

where $u(\vec{r})$ is the periodic Bloch function. The in-plane component in the QD is described by the Bessel function of the first kind Jm (pρ),

$$\varphi_{QD}(\vec{\rho}) = C_{nm} J_m(p\vec{\rho}) \qquad (2)$$

where C_{nm} is the normalization constant, p is a constant that is determined from the boundary conditions at the interface between the quantum disk and the surrounding material. In the WL, the in-plane wave function is described by the OPWs which are constructed from WL wave functions in the absence of QDs (plane waves) defined as,

$$|\psi_{WL}\rangle = \frac{1}{N_{WL}}\left[|\varphi_{WL}\rangle - \sum_{\ell}|\varphi_{QD}^{\ell}\rangle\langle\varphi_{QD}^{\ell}|\varphi_{WL}\rangle\right] \qquad (3)$$

Where the index ℓ refers to the QD state. $\varphi_{WL}(\vec{\rho})$ is the in-plane (x-y plane) quantum well WL wave function defined by,

$$\varphi_{WL}(\vec{\rho}) = \exp(i\vec{k}_{\rho}.\vec{\rho}) \qquad (4)$$

$\vec{k}_\rho$ is the in-plan WL wave vector. The normalization coefficient in Eq. (3) is defined as

$$N_{WL} = \sqrt{1 - \left| \sum_i \langle \varphi_{QD}^i | \varphi_{WL} \rangle \right|^2} \quad (5)$$

For both QD and WL, since there is an applied electric field along z-direction, their wave functions are assumed to be in the form of the Airy function. They can be written as [8],

$$\zeta(z) = \begin{cases} C_1 Ai(\eta_2) & z > -L/2 \\ C_2 Ai(\eta_1) + D_2 Bi(\eta_1) & |z| \le L/2 \\ C_3 [Bi(\eta_2) + i\, Ai(\eta_2)] & z < -L/2 \end{cases} \quad (6)$$

C_1, C_2, C_3, and D_1 are constants, Ai and Bi are the homogeneous Airy function. From the properties of Airy function, it is clear that Bi(η2) increases with increasing η2 and becomes infinity when η2 goes to infinity. In order to make the wave function well behaved in the entire region, this part is not added in the wave function in the region z > - L/2. Note that,

$$\eta_1 = -\left[\frac{2m^*}{(e\hbar F)^2}\right]^{1/3} (E_z - |e| Fz)$$
$$\eta_2 = -\left[\frac{2m^*}{(e\hbar F)^2}\right]^{1/3} (E_z - V_o - |e| Fz) \quad (7)$$

$V_o = B_{eff}[E_{gw} - E_{gd}]$ where B_{eff} is the band offset, E_{gw} and E_{gd} are the band gaps of WL and QD, respectively. F is the applied electric field, e is the electric charge and z is the associated spatial coordinate. E_z is the QD energy in the z-direction. The total QD energy is the sum of E_z with the energy obtained from the in-plane direction where its wave function is described in Eq. 2. Thus, there are differences in the calculation of the momentum matrix element between inter dot and WL-QD transitions which is taken in account.

3.2. Inter dot momentum matrix elements:

Although the application of the field in the z-direction, the momentum matrix elements are assumed only at $\hat{\rho}$ direction [11].

The momentum matrix element μ_{ij} and μ_{ii} for QD states i and j in addition to μ_{iW} for WL-QD transition and μ_{WW}. For on-diagonal elements, μ_{ii}, take μ_{11} as an example,

$$\mu_{11} = \langle \Phi_{d1} | e\rho | \Phi_{d1} \rangle = C_{mn} \int_0^a J_m(p_1\rho) J_m(p_1\rho) e\rho^2 d\rho \int_0^h \{ [C_2 A_i(\eta_1) + D_2 B_i(\eta_1)] [C_2 A_i(\eta_1) + D_2 B_i(\eta_1)] \} dz \int_0^{2\pi} \frac{e^{-im\Phi}}{\sqrt{2\pi}} \frac{e^{im\Phi}}{\sqrt{2\pi}} d\Phi \quad (8)$$

For off-diagonal elements, μ_{ij}, take μ_{12}, as an example,

$$\mu_{12} = C_{mn} \left\{ \int_0^a J_m(p_1\rho) J_n(p_2\rho) e\rho^2 d\rho \right\} \int_0^h [C_2 A_i(\eta_1, z_1) + D_2 B_i(\eta_1, z_1)] [C_2 A_i(\eta_1, z_2) + D_2 B_i(\eta_1, z_2)] dz \int_0^{2\pi} \frac{1}{2\pi} d\Phi \quad (8)$$

3.1 WL-QD momentum matrix elements:

For WL-QD transition, take μ_{34}, as an example, this momentum matrix element can be written as follows,

$$\mu_{34} = \langle \phi_{QD}^{j=3} | er | \phi_{WL} \rangle = \langle \phi_{QD}^{j=3} | e\hat{\rho}\rho | \phi_{WL} \rangle = \langle \phi_{QD}^{j=3} | e\hat{\rho}\rho | \phi_{WL} \rangle \int A_{i\_QD}(z) A_{iWL}(z) dz \quad (10-a)$$

with

$$\langle \phi_{QD}^{j=3} | e\hat{\rho}\rho | \phi_{WL} \rangle = \frac{1}{N_{WL}^2} \left[\langle \varphi_{QD}^{j=3} | e\rho | \varphi_{WL} \rangle - \sum_{i=0}^{3} \langle \varphi_{QD}^{j=3} | e\rho | \varphi_{QD}^i \rangle \langle \varphi_{QD}^i | \varphi_{WL} \rangle \right] \quad (10-b)$$

$$\langle \varphi_{QD}^{j=3} | e\rho | \varphi_{WL} \rangle = \frac{C_{mn}|e|}{\sqrt{A}} \int J_{m,j}(p\rho) e^{ik\rho} \rho^2 d\rho \quad (10-c)$$

$$\langle \varphi_{QD}^{j=3} | e\rho | \varphi_{QD}^i \rangle = C_{mn,j} C_{mn,i} |e| \int_0^{h/2} J_{m,j} \rho J_{m,i} \rho d\rho \quad (10-d)$$

For WL-WL momentum matrix element,

$$\langle \phi_{WL} | e\hat{\rho}\rho | \phi_{WL} \rangle = \frac{1}{N_{WL}^2} \left[\langle \varphi_{WL} | e\rho | \varphi_{WL} \rangle - \sum_{i=0}^{3} \langle \varphi_{QD}^i | \varphi_{WL} \rangle \langle \varphi_{WL} | e\rho | \varphi_{QD}^i \rangle \right] \quad (11)$$

$$\langle \varphi_{WL} | e\rho | \varphi_{WL} \rangle = \frac{|e|}{A} \int_0^h e^{-ik\rho} \rho e^{ik\rho} \rho d\rho \quad (12)$$

4. The Momentum Matrix under the applied optical field

4.1. Inter dot momentum matrix elements:

Although the application of the field in the z-direction, the momentum matrix elements are assumed only at ρ direction [12]. For off-diagonal elements, μ_{ij} which is the momentum matrix element μ_{ij} for QD between states i and j , take μ_{12} , as an example,

$$\mu_{12} = C_{mn}\left\{\int_0^a J_m(p_1\rho)J_n(p_2\rho)e\rho^2 d\rho\right\}A_{QD_{z1}}A_{QD_{z2}}\int_0^h \cos(k_{z_1}z)\cos(k_{z_2}z)dz\int_0^{2\pi}\frac{1}{2\pi}d\Phi \quad (13)$$

5. WL-QD momentum matrix elements

For WL-QD transition, take μ_{34} , as an example, this momentum matrix element can be written as follows:

$$\mu_{34} = \langle\phi_{QD}^{j=3}|er|\phi_{WL}\rangle = \langle\phi_{QD}^{j=3}|\hat{e\rho}\rho|\phi_{WL}\rangle$$
$$= \langle\phi_{QD}^{j=3}|\hat{e\rho}\rho|\phi_{WL}\rangle A_{QD_{z3}}A_{W_z}\int\cos(k_z z)\cos(k_{zw}z)dz \quad (14-a)$$

$$\langle\phi_{QD}^{j=3}|\hat{e\rho}\rho|\phi_{WL}\rangle = \frac{1}{N_{WL}^2}\left[\langle\varphi_{QD}^{j=3}|e\rho|\varphi_{WL}\rangle - \sum_{i=0}^{3}\langle\varphi_{QD}^{j=3}|e\rho|\varphi_{QD}^{i}\rangle\langle\varphi_{QD}^{i}|\varphi_{WL}\rangle\right] \quad (14-b)$$

$$\langle\varphi_{QD}^{j=3}|e\rho|\varphi_{WL}\rangle = \frac{C_{mn}|e|}{\sqrt{A}}\int J_{m,j}(p\rho)e^{ik\rho}\rho^2 d\rho \quad (14-c)$$

$$\langle\varphi_{QD}^{j=3}|e\rho|\varphi_{QD}^{i}\rangle = C_{mn,j}C_{mn,i}|e|\int_0^{h/2} J_{m,j}\rho J_{m,i}\rho d\rho \quad (14-d)$$

6. Results and discussion

In Table 1 the diagonal and off-diagonal elements of momentum for the double QD (DQD) structures are listed. It shows that 0.1 Debye was obtained for μ_{w0} . This refers to the effect of intermediate states in decreasing momentum.

Table (1): Calculated intraband and intersubband dipole moments for the structures studied under applied electric field.

Dipole Matrix element (Debye)	QD_1 $\rho=(14)nm$ $h=(2)nm$ QD_2 $\rho=(13)nm$ $h=(3.5)nm$ WL $h=(10)nm$	QD_1 $\rho=(14)nm$ $h=(2.5)nm$ QD_2 $\rho=(13)nm$ $h=(4)nm$ WL $h=(11)nm$	QD_1 $\rho=(14)nm$ $h=(3)nm$ QD_2 $\rho=(13)nm$ $h=(4.5)nm$ WL $h=(12)nm$	QD_1 $\rho=(14.5)nm$ $h=(2)nm$ QD_2 $\rho=(13.5)nm$ $h=(3.5)nm$ WL $h=(10)nm$	QD_1 $\rho=(15)nm$ $h=(2)nm$ QD_2 $\rho=(14)nm$ $h=(3.5)nm$ WL $h=(10)nm$
μ_{00}	2184.8	2269.3	2301.9	2186.6	2188.3
μ_{11}	2122.9	2127	2124.9	2125.4	2127.6
μ_{22}	238.5	112	68.6	250.1	258.9
μ_{33}	41	35.5	35.1	44.5	47.1

μ_{ww}	8.7528	8.7528	8.7528	8.7565	8.7593
μ_{01}	1488.3	1533.5	1548.3	1486.9	1485.5
μ_{02}	36.8	13.4	6.6	37.6	38
μ_{03}	31.5	21.1	17.8	34.7	37
μ_{12}	164.8	74.7	46.5	168.5	170.5
μ_{13}	5.2	3.9	3.5	5.7	6.1
μ_{23}	82.3	53.6	42	86.3	88.9
$\mu_{w\,0}$	0.9362	0.5724	0.1358	0.8841	0.8276
$\mu_{w\,1}$	0.7764	0.2915	0.3306	0.7343	0.6884
$\mu_{w\,2}$	4.5633	2.8746	0.3497	4.2239	3.9019
$\mu_{w\,3}$	2.4120	1.7001	0.1634	2.3642	2.2791

Fig. (1) shows the on- and off-diagonal momenta of transitions from each stat to all other states in DQD system. Fig. (1) (a) shows the momenta from state $\langle 0|$ to all other states where the momenta are reduced with increasing the distance (in units of energy) from state $\langle 0|$ to the other state. While μ_{01} is on the order of (10^3) Debye, it reduced by four orders for μ_{0w} . Fig. (1) (b) shows a similar behavior for transition between state $\langle 1|$ and other states. Fig. (1) (c) and (d) shows the effect of the intermediate states $\langle 2|$ and $\langle 3|$ where a crossing between curves was shown and the energy distance is not the controlling parameter here. Fig. (1) (e) shows the on-diagonal momenta. While μ_{00} and μ_{11} were the heighest, μ_{ww} was the smallest. The crossing was also shown for intermediate states μ_{22} and μ_{33} .

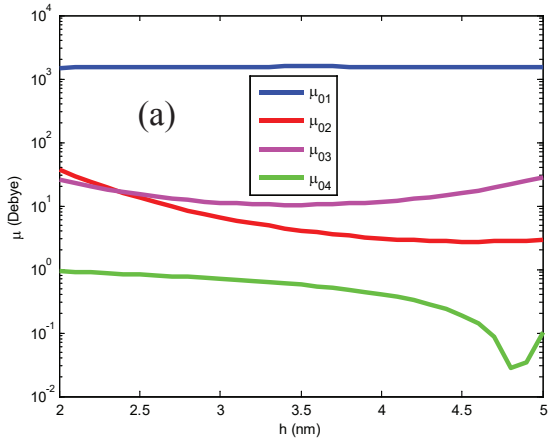

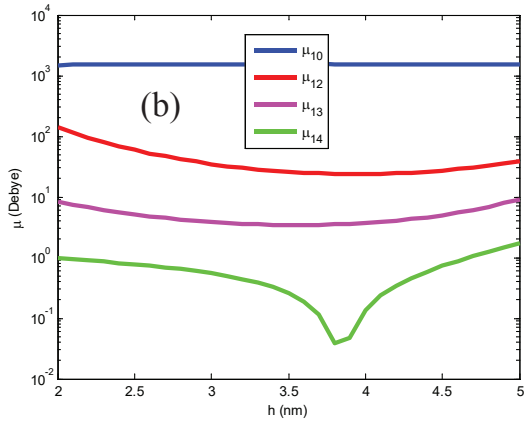

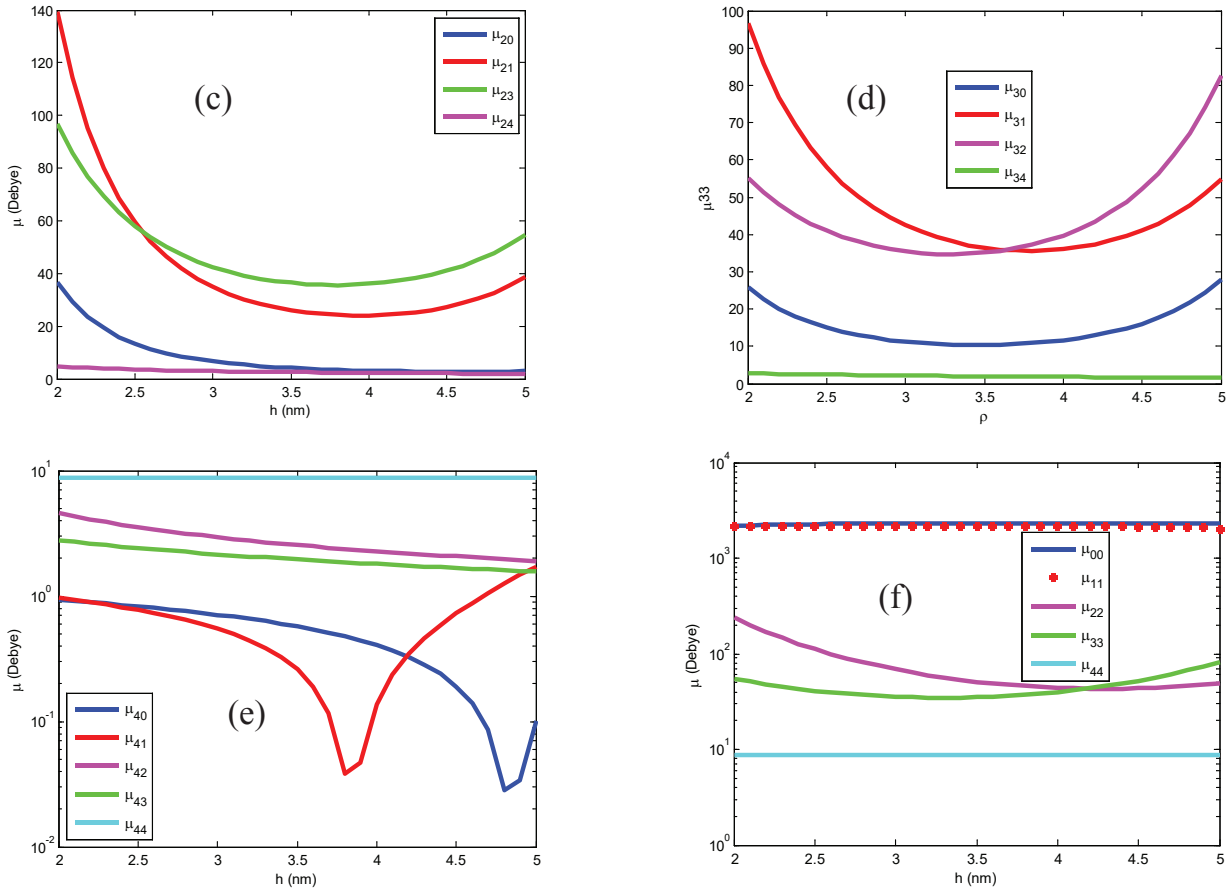

Fig. (1): Momentum matrix elements of ladder-plus-Y system: (a) transition from state $|0\rangle$, (b) from state $|1\rangle$, (c) from state $|2\rangle$, (d) from state $|3\rangle$, (e) WL-QD transitions and (f) for diagonal elements.

Fig. (2) shows on-diagonal elements of momentum versus disk radius at three values of applied electric field F= (10, 50, 100) kV/cm. While the momenta μ_{00}, μ_{22} and μ_{33} in Figs. (2) (a), (c), and (d), it is not so for μ_{11} in Fig. (2) (b). Although the momenta μ_{00}, and μ_{11} are reduced under the application of high field, the reduction is small for μ_{11}. For μ_{22} and μ_{33}, they increases under the application of high field. For all momenta in Fig. (2), the increment becomes higher for greater radius.

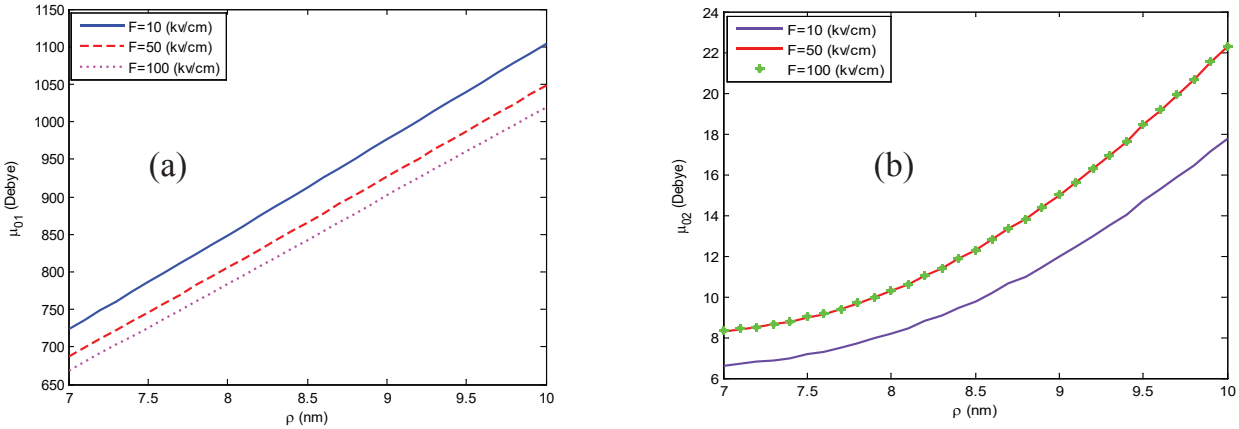

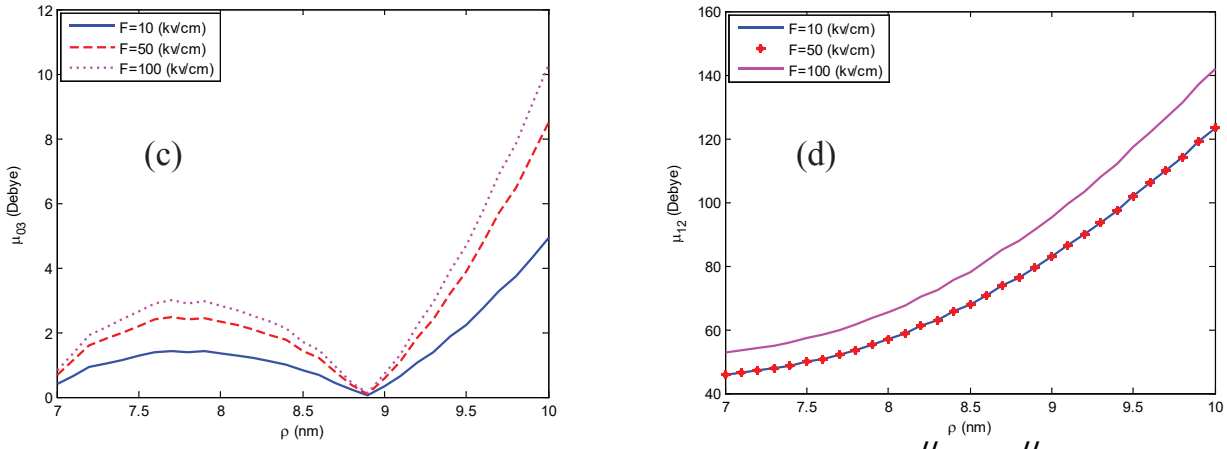

Fig. (2): On-diagonal momentum matrix elements of ladder-plus-Y system for: (a) μ_{00}, (b) μ_{11}, (c) μ_{22}, (d) μ_{33}.

Fig. (3) shows the off-diagonal elements versus disk radius under applied electric field. They shows an increment with field except μ_{01} and μ_{13} decrease with field. The increment with radius is approximately linear in diagonal elements, it is not the case here. There is an exponential growth of μ_{02} , μ_{12} , μ_{23} and a behavior of loops for μ_{03} and μ_{13}. These types of shapes may return to the energy sub bands of states results.

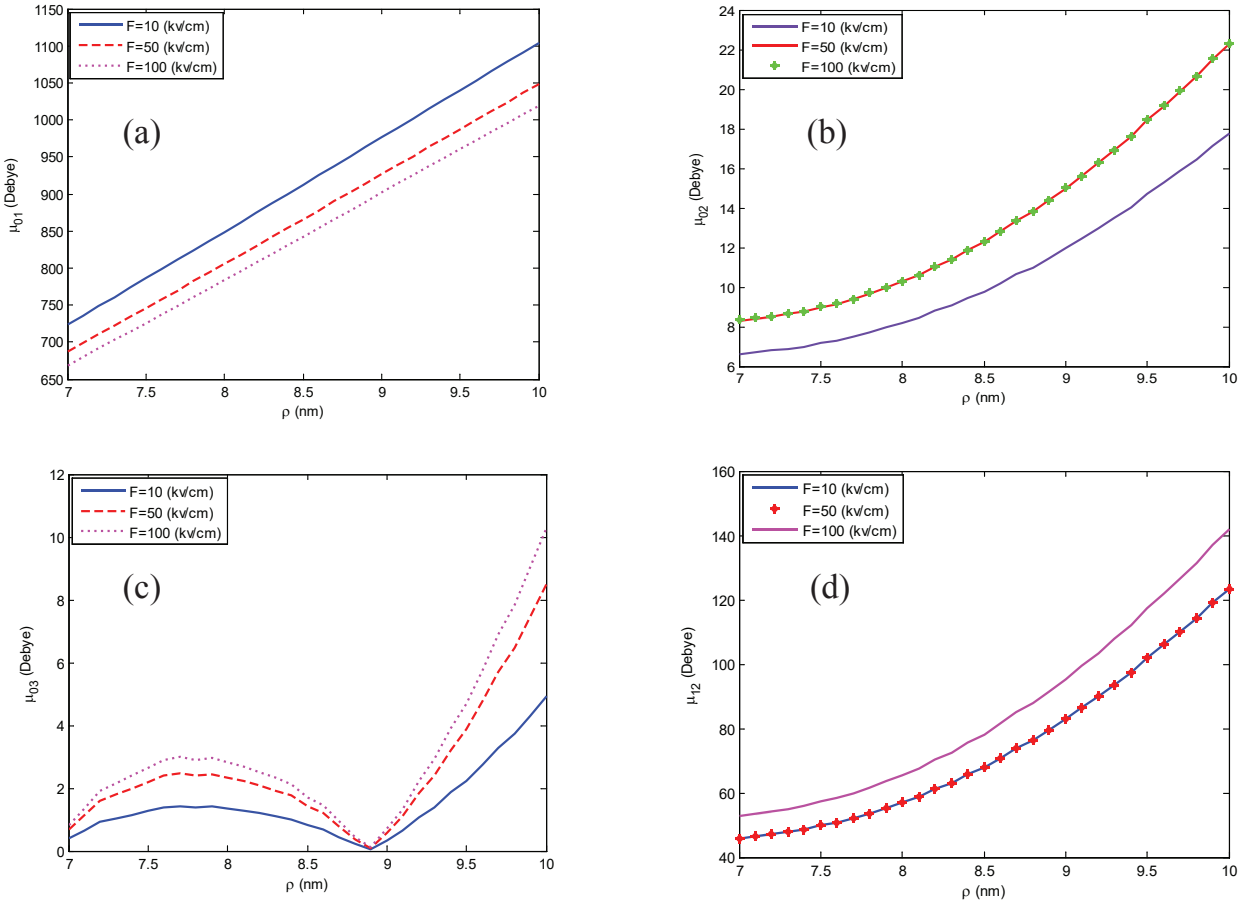

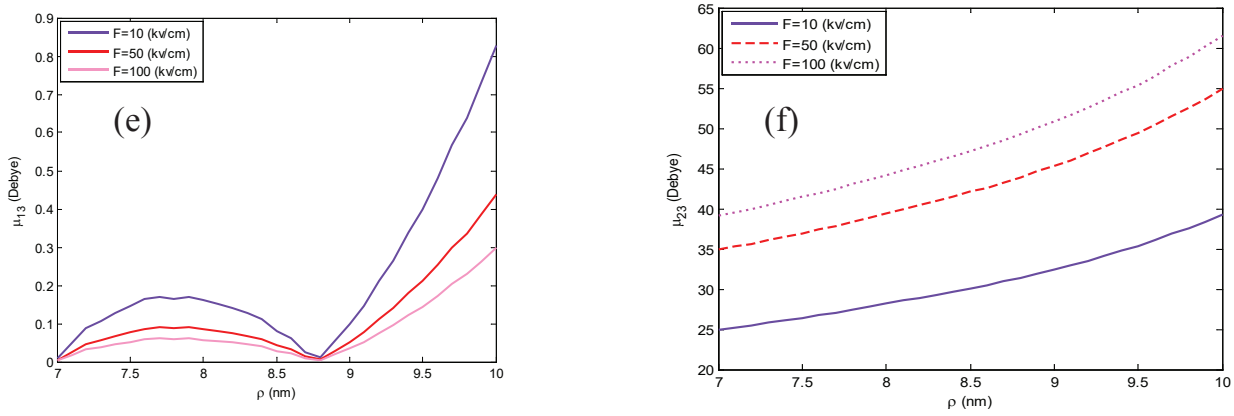

Fig. (3): Off-diagonal momentum matrix elements of ladder-plus-Y system for: (a) μ_{01}, (b) μ_{02}, (c) μ_{03}, (d) μ_{12} (e) μ_{13}, and (f) μ_{23}.

Table (2): Calculated intraband and intersubband dipole moments.

Dipole Matrix Element (Debye)	QD_1 $\rho=(14)nm$ $h=(2)nm$ QD_2 $\rho=(13)nm$ $h=(3.5)nm$ WL $h=(10)nm$	QD_1 $\rho=(14)nm$ $h=(2.5)nm$ QD_2 $\rho=(13)nm$ $h=(4)nm$ WL $h=(11)nm$	QD_1 $\rho=(14)nm$ $h=(3)nm$ QD_2 $\rho=(13)nm$ $h=(4.5)nm$ WL $h=(12)nm$	QD_1 $\rho=(14.5)nm$ $h=(2)nm$ QD_2 $\rho=(13.5)nm$ $h=(3.5)nm$ WL $h=(10)nm$	QD_1 $\rho=(15)nm$ $h=(2)nm$ QD_2 $\rho=(14)nm$ $h=(3.5)nm$ WL $h=(10)nm$
μ_{01}	514.7465	514.7465	514.7465	510.7051	506.8187
μ_{02}	299.0257	299.0257	299.0257	321.6688	340.4747
μ_{03}	227.7338	227.7338	227.7338	259.3194	285.5862
μ_{12}	338.6227	338.6227	338.6227	361.9331	381.5335
μ_{13}	261.9817	261.9817	261.9817	294.9830	322.6829
μ_{23}	484.9196	484.9196	484.9196	500.3586	514.1616
$\mu_{w\,0}$	25.6488	25.6488	25.6488	26.9734	28.0888
$\mu_{w\,1}$	28.6170	28.6170	28.6170	30.0063	31.1900
$\mu_{w\,2}$	31.2383	31.2383	31.2383	33.4176	35.2821
$\mu_{w\,3}$	27.9814	27.9814	27.9814	30.5059	32.7057

(e)

Table (2) shows an example of calculated moments at QD and WL sizes for some DQD structure. From the table, the highest momentum was μ_{10} while the lowest momenta are for WL-QD transitions. Of course this is because the difficulty of transition between the dissimilar WL and QD layers. It was referred earlier to the transition difficulty between QD and other dissimilar layers where the bottleneck effect was considered between these different layers [13].

Conclusions

In this work, on- and off-diagonal momentum matrix elements of QD structure under the application of (and without) applied electric field were modeled for the structure layers; QD layer and WL considering OPW for in-plane WL states.

While there is a definite size gives maxima for off-diagonal elements, the on-diagonal elements under applied field increases with size. Some of on-diagonal elements increases with field while some other decreases. QD-WL transitions have the lowest momenta.

Known of these tramsition elements was important in optical, quantum opitcs, and all-optical applications.

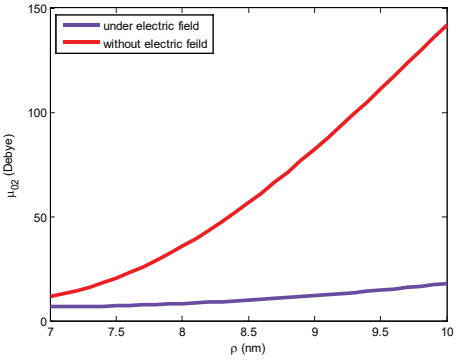

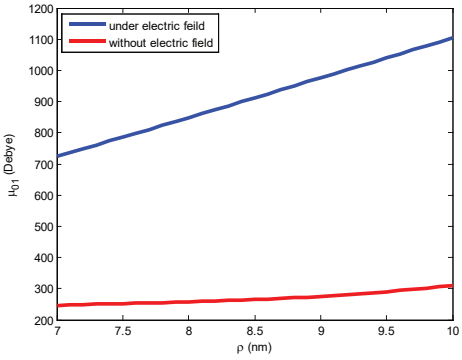

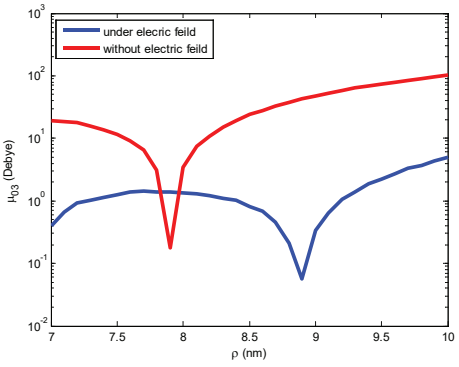

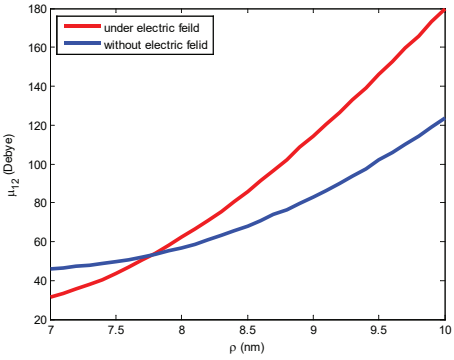

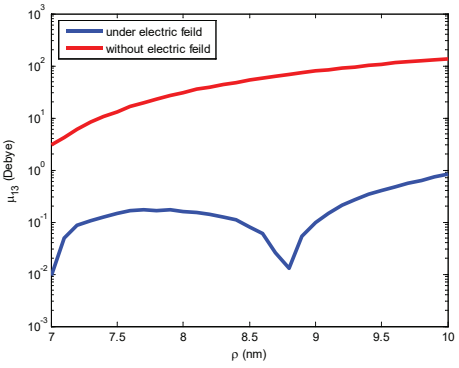

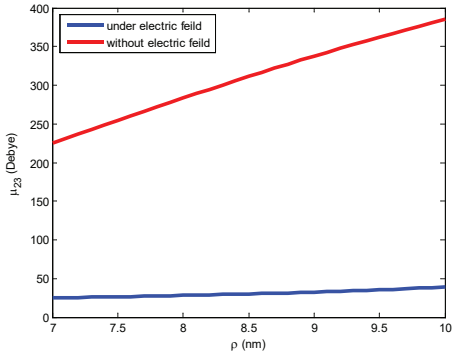

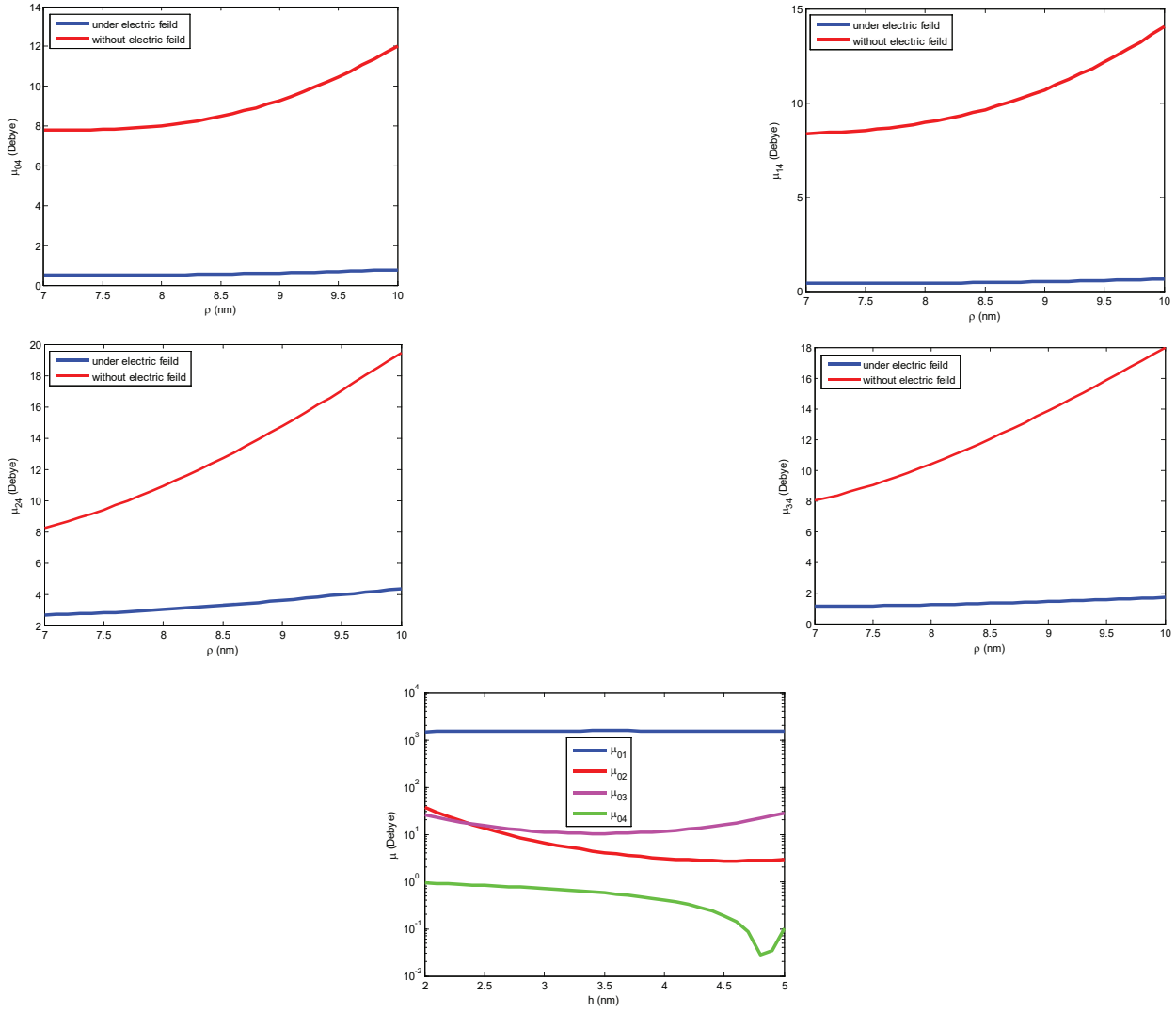

Fig. (4): Momentum matrix elements of ladder-plus-Y system.

References

[1] C. Dane, H. Akbas, S. Minez, A. Guleroglu, Physica E 41 278–281(2008).

[2] J. Kim and Sh. L. Chuang, IEEE J. of Quantum Electronics (2006).

[3] A. Enshaeian, G. Rezaei, S. F. Taghizadeh, Proceedings of the 4th International Conference on Nanostructures (ICNS4) 12-14 March, Kish Island, I.R. Iran, (2012).

[4] D. Ahn and S. L. Chuang, Physical Review B 34 9034-9037, (1986).

[5] D. Ahn and S.L. Chuang, IEEE J. Quantum Electronics 23 2196-2204, (1987).

[6] Z. Li and X. Hong-Jing, Commun. Theor. Phys. 41 761-766, (2004).

[7] B. I. Lembrikov, and M. Haridim Y. Ben-Ezra, IEEE J. Quantum Electrons 41, 1268-1273, (2005).

[8] M. Abdullah, F. T. M. Noori and Amin H. Al-Khursan, Appl. Opt. 54 5168-5192, (2015).

[9] E. Malic, M. J. P. Bormann, P. Hovel, M. Kuntz, D. Bimberg, A. Knorr, and E. Scholl, IEEE Selected Topics Quantum Electronics 131242-1248, (2007).

[10] T. R. Nielsen, P. Gartner, and F. Jahnke, Phys. Rev. B 69 235314, (2004).

[11] J. Kim1, S. L. Chuang, P. C. Ku and C. J. Chang-Hasnain, J. Phys. D 16 S3727–S3735, (2004).

[12] A. Zrenner, E. Beham, S. Stufler, F. Findeis, M. Bichler and G. Abstreiter, Nature 418, 612-614,(2002).

[13] A. H. Al-Khursan, Journal of Luminescence 113, 129-136, (2005).